

FIRST LIGHT FOR THE FIRST STATION OF THE LONG WAVELENGTH ARRAY

G. B. TAYLOR^{*,†,****}, S. W. ELLINGSON[‡], N. E. KASSIM[§], J. CRAIG^{*}, J. DOWELL^{*},
C. N. WOLFE[‡], J. HARTMAN^{¶,||}, G. BERNARDI^{**}, T. CLARKE[§], A. COHEN^{††}, N. P. DALAL^{‡‡},
W. C. ERICKSON^{§§}, B. HICKS[§], L. J. GREENHILL^{**}, B. JACOBY^{¶¶}, W. LANE[§], J. LAZIO[¶],
D. MITCHELL^{|||}, R. NAVARRO[¶], S. M. ORD^{**}, Y. PIHLSTRÖM^{*}, E. POLISENSKY[§],
P. S. RAY[§], L. J. RICKARD^{*}, F. K. SCHINZEL^{*}, H. SCHMITT^{***}, E. SIGMAN[¶], M. SORIANO[¶],
K. P. STEWART[§], K. STOVALL^{†††}, S. TREMBLAY^{‡‡‡,§§§}, D. WANG[¶], K. W. WEILER[§],
S. WHITE^{¶¶¶} and D. L. WOOD^{|||}

^{*}Department of Physics and Astronomy, University of New Mexico
Albuquerque NM, 87131, USA

[†]Greg Taylor is also an Adjunct Astronomer at the
National Radio Astronomy Observatory

[‡]Bradley Department of Electrical and Computer Engineering
Virginia Polytechnic Institute and State University
Blacksburg, VA 24061, USA

[§]U.S. Naval Research Laboratory
Washington, DC 20375, USA

[¶]NASA Jet Propulsion Laboratory
Caltech Institute of Technology, Pasadena, CA 91109, USA

^{||}NASA Postdoctoral Program Fellow

^{**}Harvard-Smithsonian Center for Astrophysics
60 Garden St., Cambridge, MA 02138, USA

^{††}Johns Hopkins University Applied Physics Laboratory Laurel
MD 20723, USA

^{‡‡}Northrup Grumman, Aerospace Systems
Redondo Beach, CA 90278, USA

^{§§}University of Tasmania
Hobart, Australia

^{¶¶}Affiliated with The Aerospace Corporation
Chantilly, VA 20151, USA

^{|||}University of Melbourne, Australia

^{***}Computational Physics, Inc.
Springfield, VA 22151, USA

^{†††}Center for Gravitational Wave Astronomy and
Department of Physics and Astronomy, University of Texas at Brownsville
Brownsville, TX 78520, USA

^{‡‡‡}ARC Centre of Excellence for All-Sky Astrophysics (CAASTRO)

^{§§§}International Centre for Radio Astronomy Research, Curtin University
Bentley WA, Australia

^{¶¶¶}Space Vehicles Directorate, AFRL
Albuquerque, NM, USA

^{|||}Praxis, Inc., Alexandria, VA 22303, USA

^{****}gbtaylor@unm.edu

Received 2012 March 19; Revised 2012 June 27; Accepted 2012 June 27; Published 2012 August 7

The first station of the Long Wavelength Array (LWA1) was completed in April 2011 and is currently performing observations resulting from its first call for proposals in addition to a continuing program of commissioning and characterization observations. The instrument consists of 258 dual-polarization dipoles, which are digitized and combined into beams. Four independently-steerable dual-polarization beams are available, each with two tunings of 16 MHz bandwidth that can be independently tuned to any frequency between 10 MHz and 88 MHz. The system equivalent flux density for zenith pointing is ~ 3 kJy and is approximately independent of frequency; this corresponds to a sensitivity of ~ 5 Jy/beam (5σ , 1 s); making it one of the most sensitive meter-wavelength radio telescopes. LWA1 also has two “transient buffer” modes which allow coherent recording from all dipoles simultaneously, providing instantaneous all-sky field of view. LWA1 provides versatile and unique new capabilities for Galactic science, pulsar science, solar and planetary science, space weather, cosmology, and searches for astrophysical transients. Results from LWA1 will detect or tightly constrain the presence of hot Jupiters within 50 parsecs of Earth. LWA1 will provide excellent resolution in frequency and in time to examine phenomena such as solar bursts, and pulsars over a 4:1 frequency range that includes the poorly understood turnover and steep-spectrum regimes. Observations to date have proven LWA1’s potential for pulsar observing, and just a few seconds with the completed 256-dipole LWA1 provide the most sensitive images of the sky at 23 MHz obtained yet. We are operating LWA1 as an *open skies* radio observatory, offering ~ 2000 beam-hours per year to the general community. At the same time, we are operating a backend for all-sky imaging and total-power transient detection, approximately 6840 hours per year ($\sim 78\%$ duty cycle).

Keywords: Sun, Jupiter, pulsars, extrasolar planets, Dark Ages, long wavelength instrumentation.

1. Introduction to LWA1

LWA1 originated as the first “station” (beam-forming array) of the Long Wavelength Array (LWA). The LWA concept was conceived by Perley & Erickson (1984) and expanded by Kassim & Erickson (1998) and Kassim *et al.* (2005). It gained momentum with sub-arcminute imaging with the VLA at 74 MHz (Kassim *et al.*, 1993, 2007a) and the project began in earnest in April 2007, sponsored primarily by the Office of Naval Research (ONR), with the ultimate goal of building an aperture synthesis radio telescope consisting of 53 identical stations distributed over the U.S. Southwest (Ellingson *et al.*, 2009, 2011). Currently, the LWA project exists as a collaboration, which we refer to as the Long Wavelength Array Collaboration (LWAC). The LWAC is an informal “umbrella” organization which serves to facilitate collaboration among organizations, projects, and individuals with LWA-related interests. The LWAC has no legal identity, no specific charter, and no dedicated funding; membership is completely open and it exists solely to facilitate collaboration among its members. The LWAC coordinator is currently N. E. Kassim of the U. S. Naval Research Laboratory. The LWAC currently includes the following projects:

- LWA1: Originally conceived as the first station of the LWA, but which is now a dedicated radio telescope distinct from (but supportive of) the separate effort to build a long-baseline aperture synthesis instrument. The topic of this paper.

- LoFASM; an initiative by the University of Texas at Brownsville (UTB), PI R. Jenet, to build and deploy three or more “mini-stations” for the purpose of monitoring the sky for transient sources.
- Cosmic Dawn; a project to measure, or place constraints, on the HI signal from the Dark Ages using beamforming data from LWA1. This effort is being led by J. Bowman.
- LEDA (“Large aperture Experiment to detect the Dark Ages”); an initiative to develop an alternative backend for LWA1 led by L. Greenhill. Additional information about LEDA is provided in Sec. 2.4.
- LWA; the continuing initiative to fund and build a 53-station long-baseline aperture synthesis instrument.

Institutions represented in the LWAC (as determined by attendance at the May 12, 2011 LWA1 User Meeting) include U.S. Air Force Research Laboratory (AFRL), Arizona State University (ASU), Harvard University, Kansas University (KU), Long Island University, National Radio Astronomy Observatory (NRAO), NASA Jet Propulsion Laboratory (JPL), U.S. Naval Research Laboratory (NRL), New Mexico Tech (NMT), University of New Mexico (UNM), University of Texas at Brownsville (UTB), and Virginia Tech (VT). New institutions and individuals are invited to join the LWAC and if interested should contact Namir Kassim (NRL) or Greg Taylor (UNM).



Fig. 1. Aerial view of the LWA1 radio observatory.

The LWA1 Radio Observatory is shown in Fig. 1. It is located on NRAO land within the central square mile of the VLA, which offers numerous advantages. The project to design and build LWA1 was led by UNM, who also developed analog receivers and the shelter and site infrastructure systems. The system architecture was developed by VT, who also developed LWA1's monitor & control and data recording systems. Key elements of LWA1's design were guided by experience gained from a prototype stub system project

known as the Long Wavelength Demonstrator Array, developed by NRL and the University of Texas at Austin (York *et al.*, 2007); and by VT's Eight-meter wavelength Transient Array (ETA; Deshpande, 2009). NRL developed LWA1's active antennas, and JPL developed LWA1's digital processing subsystem. LWA1 has recently been established as a University Radio Observatory by NSF and as such will make regular calls for proposals from the astronomical community starting in February 2012. Table 1 summarizes the capabilities

Table 1. Summary of LWA1 specifications.

| Specification | As built description |
|--------------------------|--|
| Beams: | 4, independently-steerable, each dual-polarization |
| Tunings: | 2 independent center frequencies per beam |
| Freq Range: | 24–87 MHz (>4:1 sky-noise dominated); 10–88 MHz usable |
| Instantaneous bandwidth: | $\leq 16 \text{ MHz} \times 4 \text{ beams} \times 2 \text{ tunings}$ |
| Minimum channel width: | ~ 0 (No channelization before recording) |
| Beam FWHM: | $[8, 2]^\circ$ at [20, 80] MHz for zenith-pointing |
| Beam SEFD: | $\sim 3 \text{ kJy}$ (approximately frequency-independent) zenith-pointing |
| Beam Sensitivity: | $\sim 5 \text{ Jy}$ (5σ , 1 s, 16 MHz) for zenith-pointing |
| All-Dipoles Modes: | TBN: 75 kHz bandwidth continuously from every dipole TBW: Full band (78 MHz) every dipole for 61 ms, once every ~ 5 min. |

of LWA. For more details see the LWA web pages at <http://lwa.unm.edu> including the LWA Memo series.

Given the architectural similarities to a LOFAR low band array (LBA) station (de Vos, Gunst & Nijboer, 2009), it is appropriate to identify key similarities and differences. LOFAR is an operational radio telescope array based in the Netherlands with frequency coverage overlapping that of LWA1. AART-FAAC (www.aartfaac.org) is a planned imaging-based search for radio transients with LOFAR, using a correlator which is currently under development. An approximate comparison of the sensitivity of LOFAR and LWA1, based on information provided in Wijnholds & van Cappellen (2011), proceeds as follows: LWA1 has 258 dual-polarized dipoles (or “stands”), whereas LOFAR currently has 36 stations consisting of 96 dual-polarized dipoles each, of which only 48 can be used simultaneously, for a total of 1728 dual-polarized dipoles. However, LWA1 per-dipole system temperature is dominated by Galactic noise by a factor of at least 4:1, whereas LOFAR per-dipole system temperature is at best 1:1. Taking this into account, we estimate all of LOFAR is more sensitive than LWA1 by a factor of no greater than ~ 4 on a per-bandwidth basis, at LOFAR’s optimum frequency (~ 60 MHz). We also note that LWA1 (34°N) sees a significantly different portion of the sky than

LOFAR ($\sim 52^\circ\text{N}$), including access to the interesting Galactic center and inner plane regions. A graphical comparison of LWA1 with LOFAR and other contemporaneous instruments is shown in Fig. 2.

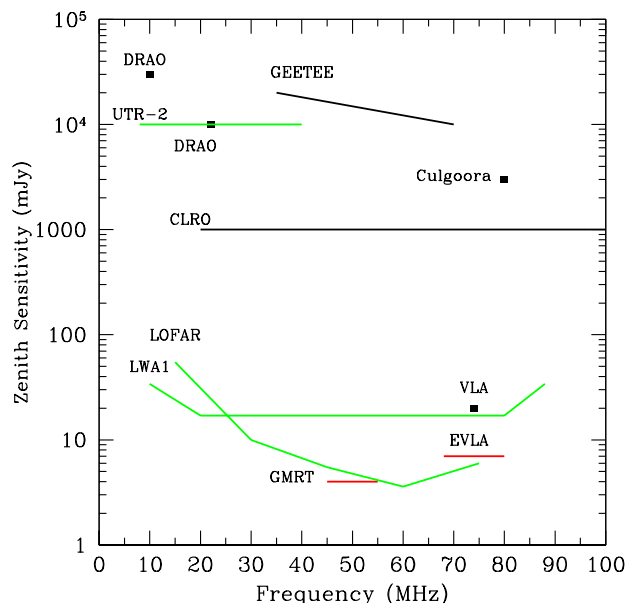


Fig. 2. (Color online) Sensitivity of the LWA1 compared to other instruments. Integration time is 1 hr for all instruments and the bandwidths assumed for current and planned instruments (green and red respectively) are as follows: UTR2: ~ 3 MHz, LOFAR: 16 MHz, Y=VLA: 3 MHz, LWA1: 16 MHz, GMRT: 10 MHz. No effects of confusion noise are considered.

Table 2. Glossary of LWA1 terms.

| Term | Description |
|---------|---|
| CARC | The UNM Center for Advanced Research Computing |
| CFP | Call for Proposals |
| CGP | Crab Giant Pulses |
| DRSU | Data Recorder Storage Unit (a 10 TB eSATA drive array used by LWA1 data recorders) |
| IOC | Initial Operational Capability |
| LDA | LWA1 Data Archive (see Sec. 4) |
| LEDA | Large aperture Experiment to detect the Dark Ages, a new backend for LWA1 |
| LSL | LWA Software Library; a collection of software for reading and analyzing LWA data |
| LWA | Long Wavelength Array; a future aperture synthesis radio telescope consisting of 53 stations similar to LWA1 |
| LWAC | LWA Collaboration |
| LWA1 | The first LWA station, now operating as a single-station radio observatory |
| LWANA | The LWA North Arm Stub Station located near the end of the VLA’s North Arm (Sec. 3) |
| MCS | Monitor and Control System, the software and computers that control LWA1 |
| PASI | Prototype All-Sky Imager (an existing backend for LWA1) |
| Stands | A pair of orthogonally-aligned active dipoles sharing a mast |
| Station | An antenna array and associated electronics. Analogous to a single dish, except able to point beams in multiple directions simultaneously |
| TBN | Transient Buffer Narrowband (an LWA1 “all sky” observing mode) |
| TBW | Transient Buffer Wideband (an LWA1 “all sky” observing mode) |

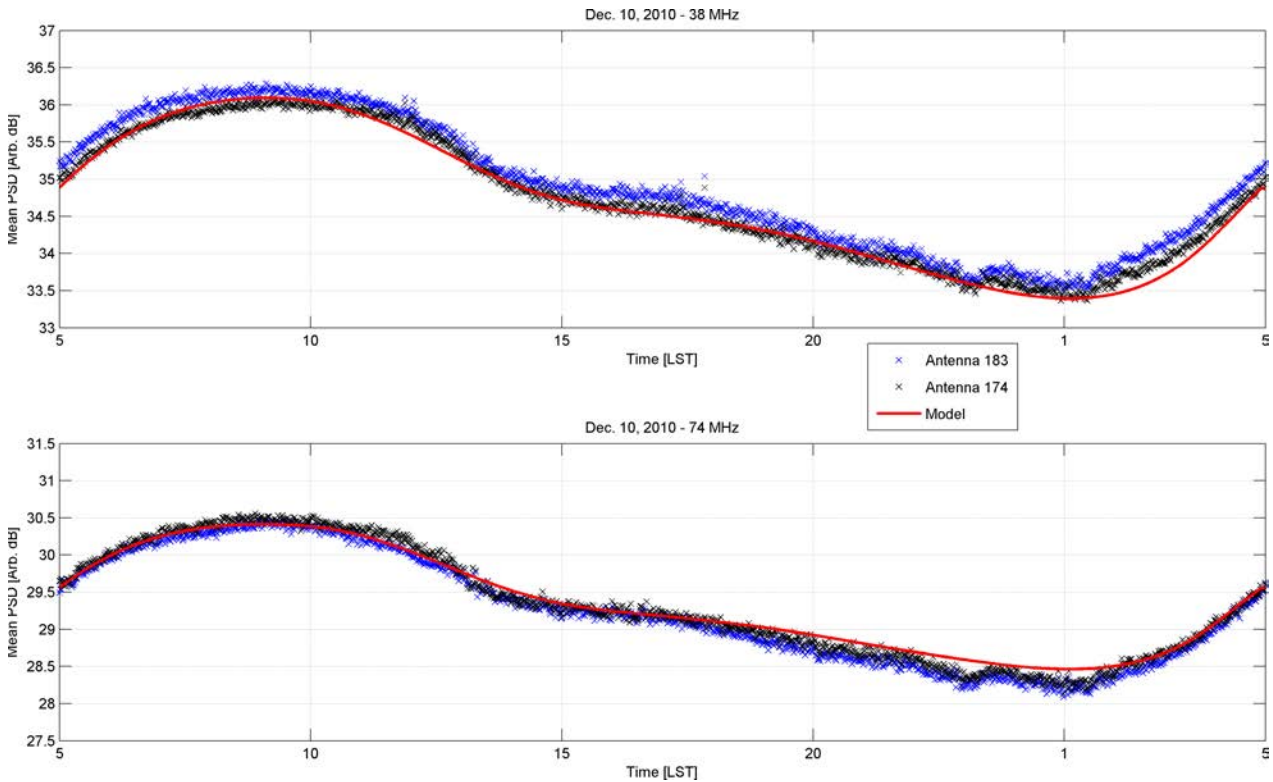


Fig. 3. (Color online) Dipole total power measurements (1 MHz bandwidth, 61 ms integration per point). Variation is due to the changing sky brightness temperature distribution as seen by the dipole. The solid red line is our prediction obtained by convolving the sky model of de Oliveira-Costa *et al.* (2008) with a model of the dipole pattern obtained from electromagnetic simulation. No RFI mitigation or editing has been applied.

For the convenience of the reader, Table 2 provides a glossary of some of the more arcane acronyms associated with LWA1.

At the time of this writing, science observations have begun while commissioning continues. We anticipate reaching IOC (“initial operational capability”) — essentially the beginning of routine operation as an observatory — in Spring 2012. We now summarize some early results obtained during commissioning. Figure 3 shows single dipole total power for a period of 24 hrs at 38 and 74 MHz for two antennas. The dipole power measurements compare well with a model of the expected power derived from a sky model convolved with the calculated antenna pattern. The agreement confirms that we are strongly sky noise-dominated ($>4:1$ from 24–87 MHz), that we have a good understanding of our dipole responses, and that RFI is manageable.

We have begun imaging the sky with LWA1. In Fig. 4 we show three views of the sky taken with the Transient Buffer Narrowband (TBN) mode on May 16, 2011 using 210 stands (21945 baselines). In these Stokes I images one can see the Galactic plane,

Cas A, and Tau A, and at the lowest frequency Jupiter is quite prominent. LWA1 routinely images the sky in near real-time using the Transient Buffer Narrowband (TBN) capability of the station and a modest cluster located at LWA1. These images are shown live on “LWA-TV” which is available from the LWA web pages.^(a) Time-lapse movies of the day’s images are also made available at the end of each day.

In Fig. 5 we show a spectrogram obtained from TBW data taken over 24 hrs for a 20-dipole zenith-pointing beam. The integration time of the individual captures is 61 ms, and one capture was obtained every minute. The frequency resolution is ~ 10 kHz. The diurnal variation noted in Fig. 3 is apparent here as well. Strong RFI from the FM bands shows up as vertical lines at 88 MHz and above. Below 30 MHz there are a variety of strong communications signals. While there is abundant RFI visible in the spectrum, it is very narrowband, obscures only a tiny fraction of our band, and does

^a<http://www.phys.unm.edu/lwa/lwatv.html>.

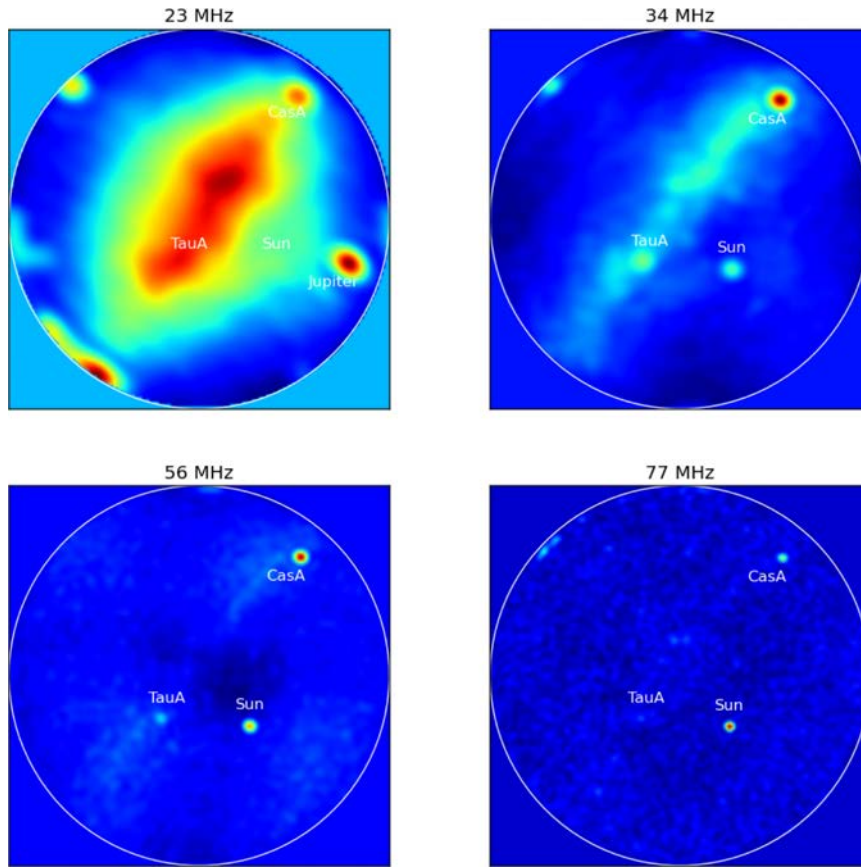


Fig. 4. Nearly-simultaneous all-sky images taken at 4 widely separated frequencies using LWA1’s TBN mode. Absolute calibration is the same in all four images; the apparent decrease in sky brightness with increasing frequency is real, and the bright region near zenith is the Galactic plane. Clearly visible at 23 MHz is Jupiter, and the horizon “hot spots” in the 23 MHz image are ionospherically-refracted RFI. Note that Cas A and the Sun are visible in all images. Data was obtained for 10 s each, 50 kHz bandwidth, using 210 stands.

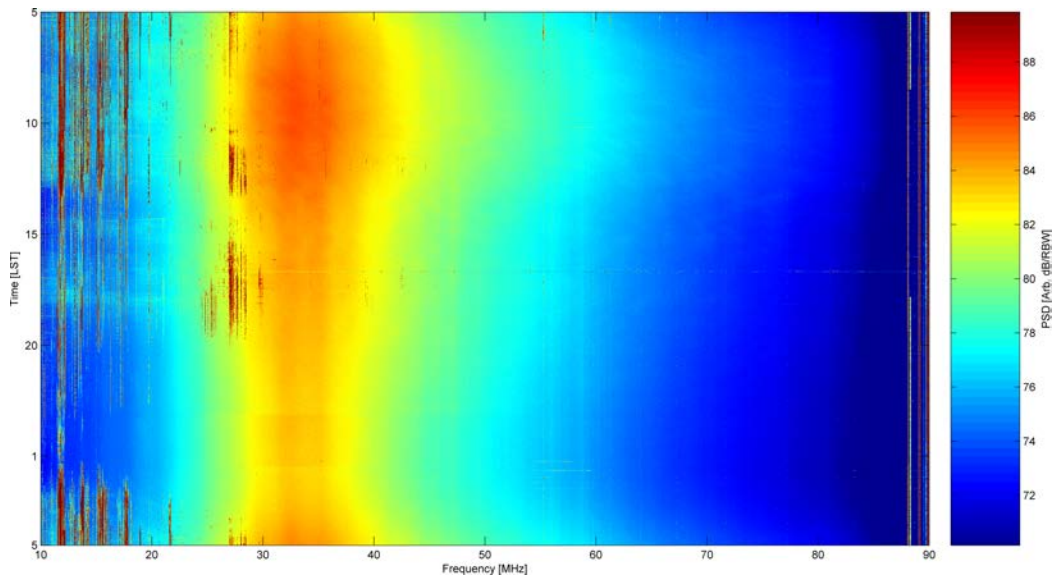


Fig. 5. Spectrum using the TBW capture mode for 20 dipoles phased at zenith for 24 hrs. The time and frequency variation of the background are real; the contribution of the active antenna appears as a steep roll-off below 30 MHz. Note that 30–88 MHz is always useable, and even frequencies as low as 13 MHz are usable for a few hours each day.

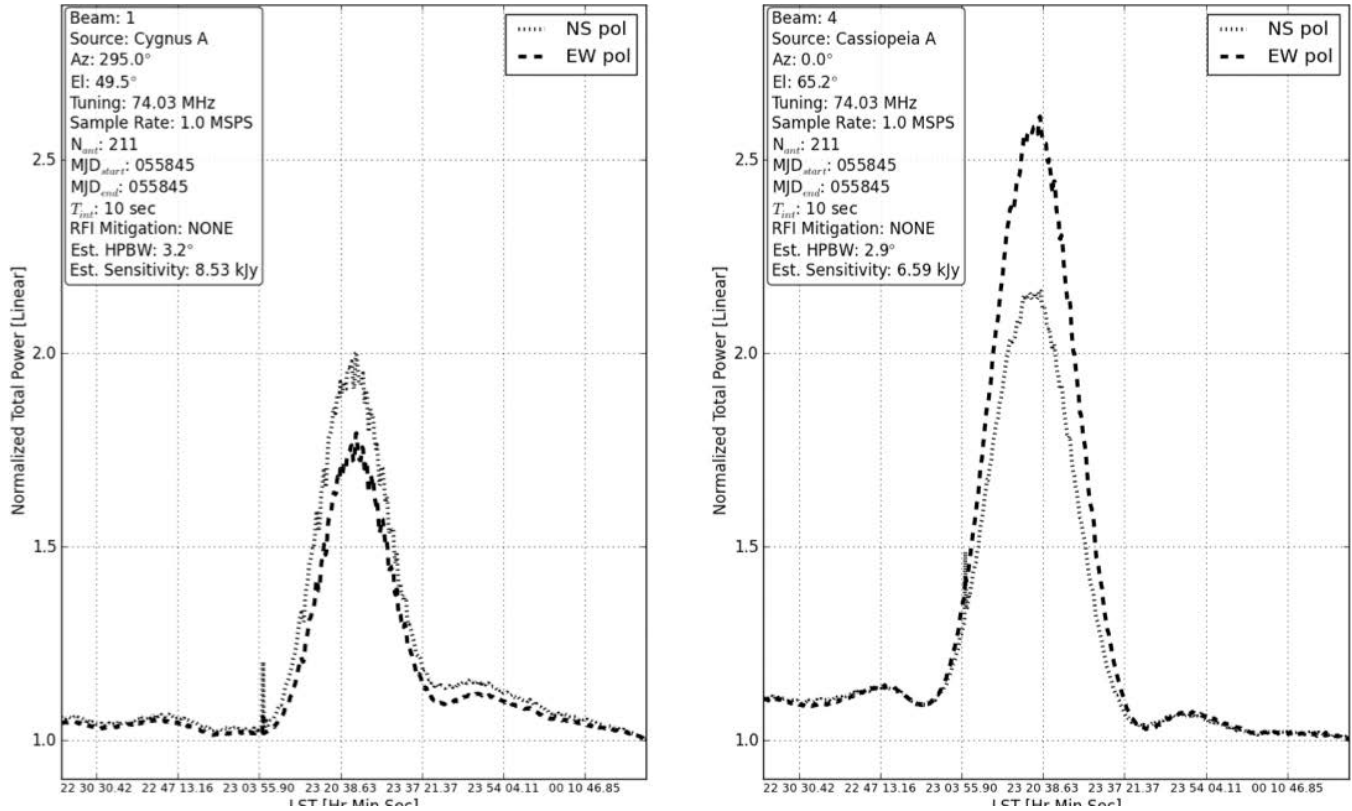


Fig. 6. Simultaneous observations of Cyg A and Cas A using two of the four LWA1 beams at 74 MHz with a 1 MHz bandwidth.

not interfere with our ability to be sky-noise limited. More details about the RFI environment can be found in Obenberger & Dowell (2011).

LWA1 supports the formation of up to 4 simultaneous beams. In Fig. 6 we illustrate the formation of two simultaneous beams, one placed on Cassiopeia A and one placed on Cygnus A. No tracking was performed so the two sources drift through the beam. One can see the response of the beam to Galactic emission as well as to Cygnus A and Cassiopeia A. The two sources have roughly equal flux density at 74 MHz (17 kJy; Helmboldt & Kassim 2009), so the observed difference is primarily a result of the different dipole patterns at their respective elevations.

Figure 7 demonstrates that with very simple RFI mitigation, LWA1’s sensitivity is limited by noise alone — as opposed to RFI or instrumental stability — for integrations up to many hours. Note that we have made no deliberate attempt in Fig. 7 to correct for instrumental stability (e.g., calibration against a noise standard), and that

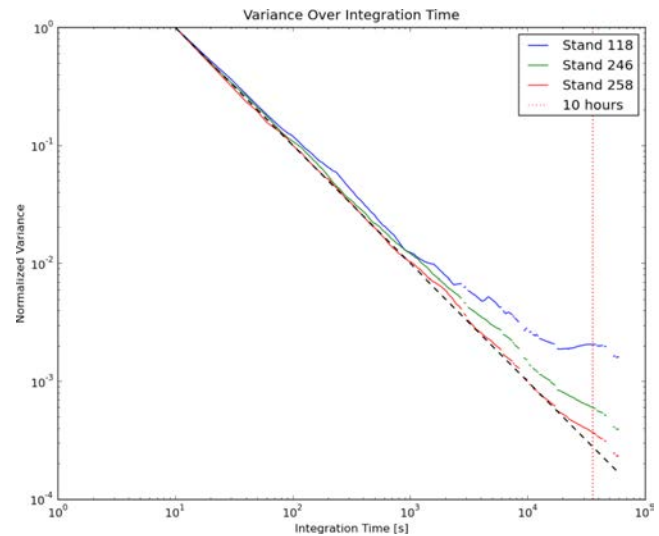


Fig. 7. Variance over time using a ~ 50 kHz bandwidth and 2048 channels at 38 MHz for three dipoles. The black dashed line shows the expectation of variance falling as the square root of integration time. The vertical bar marks 10 hours. Crude RFI excision was performed by discarding $\sim 20\%$ of the channels (in practice $< 1\%$ is generally sufficient).

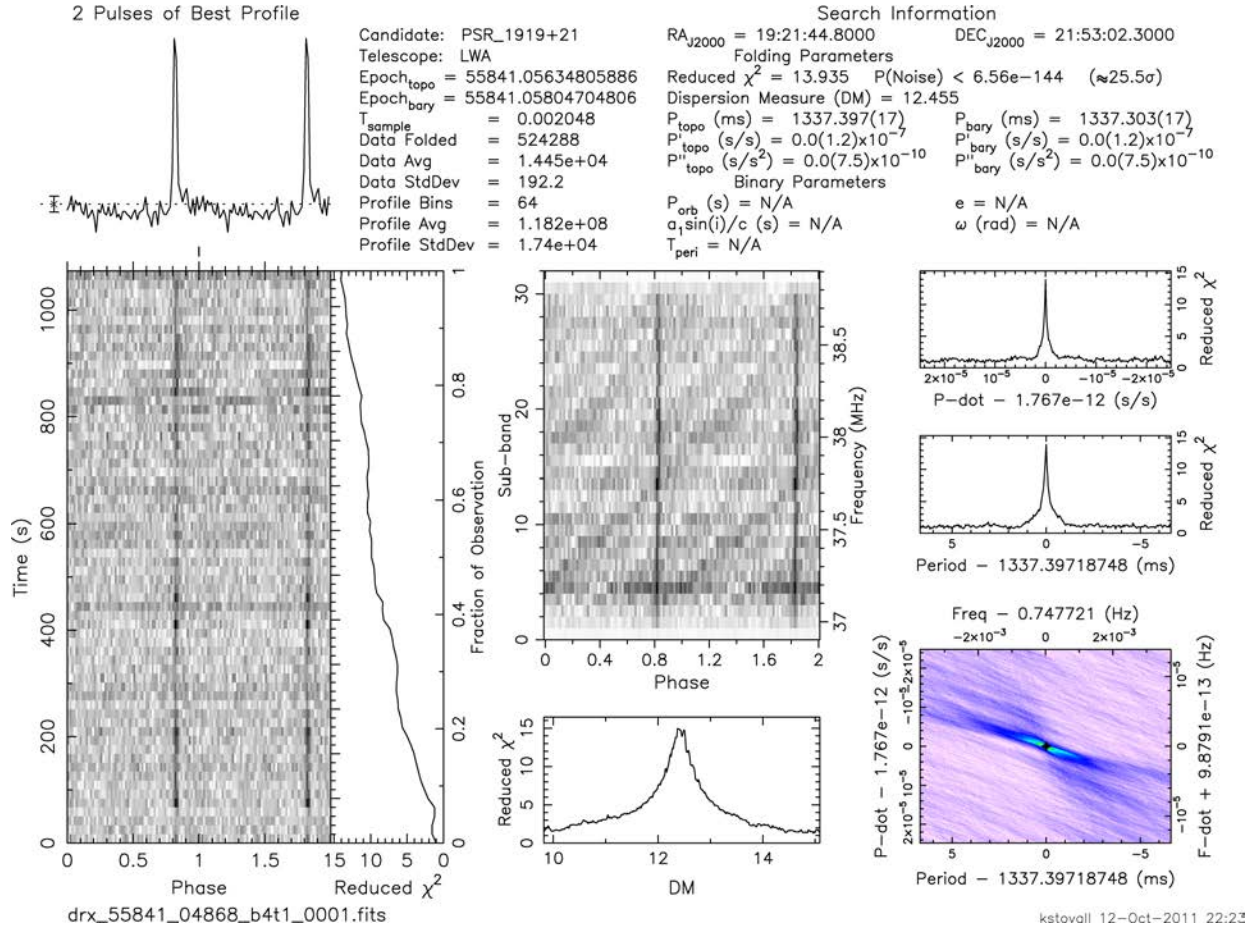


Fig. 8. First LWA1 detection of the pulsar B1919+21 in a 1 MHz beam taken during commissioning observations. The pulsar observations were processed using PRESTO (Ransom, 2001). The panels are: (bottom left) plot of pulsar phase vs. observation length averaged into 0.13 second bins; (top left) integrated pulse profile dedispersed at optimal signal strength; (top right) χ^2 as a function of trial \dot{P} at optimal P and DM ; (middle right) χ^2 as a function of trial P at optimal DM and \dot{P} ; (bottom right) Reduced χ^2 surface of trial P and \dot{P} at optimal DM ; (bottom middle) χ^2 as a function of trial DM at optimal P and \dot{P} ; (top middle) Plot of pulse phase vs. observing frequency. Data was folded at optimal P and \dot{P} for the entire dataset for a particular sub-band (frequency range). In this case there are 32 frequency sub-bands. These sub-bands are then plotted with dedispersion accounted for in order to show that the pulsar was seen throughout the observed frequency range.

doing so can be expected to result in even better performance.

In Fig. 8 we show the pulse profile from B1919+21, a strong, long period, low dispersion measure pulsar. This was one of the first observations with the beamforming mode of LWA1, and not only confirms the ability of LWA1 to do leading-edge pulsar science, but also demonstrates that digital beamforming is working properly.

2. Scientific Program

With the ability to point in several directions at once, wide fractional bandwidths, and large collecting area, the first LWA station will make important scientific contributions in several fields.

We have been refining the science case for LWA1 over 5 years — see Kassim *et al.* (2006, 2010), Clarke *et al.* (2009), Rickard *et al.* (2010), and Lazio *et al.* (2010) for details. Projects granted observing time in the first (primarily internal) call for proposals cover a range of topics including pulsars, transients, cosmology, Galactic science, the Sun, and the Earth’s ionosphere (see Table 3). Below we elaborate upon several of these topics and the headway that LWA1 will soon make in each.

2.1. Pulsars

Pulsars are fascinating objects with spin periods and magnetic fields strengths ranging over 4 and 5 orders of magnitude respectively. Though it is well

Table 3. LWA1 approved observing projects.

| Project title | Beam hours | TB hours | PI | PI Affil. | Co-I |
|--|---------------|-------------|---------------|--------------|-----------------------------|
| LWA Cosmic Ray Air Shower Trigger | | 144 | D. Besson | KU | UNM |
| Tracking the Dynamic Spectrum of Jupiter | 56 | 20 | T. Clarke | NRL | MTSU, UNM, NRAO, UTas |
| Ionospheric Scintillation | 344 | | P. Crane | NRL | UCSD |
| Passive Meteor Scatter using the Long Wavelength Array | 40 | 20 | S. Close | Stanford | PSU, Stanford |
| A GCN-Triggered Search for GRB Prompt Emission | 320 | | S. Ellingson | VT | |
| Crab Giant Pulses | 640 | | S. Ellingson | VT | JPL, NRL, Swinburne |
| Continuing Measurements of the Cas A/Cyg A Flux Ratio | 6 | | J. Hartman | NRL | |
| Searching for Hot Jupiters with LWA1 | 300 | | J. Hartman | NRL | UCB |
| Carbon Radio Recombinations Lines in the Cygnus Arm | 378 | | Y. Pihlström | UNM | NRL, UTas |
| Multi-frequency Large Scale Sky Survey | 672 | | E. Polisensky | NRL | UTas |
| Low Frequency Studies of Radio Pulsars | 50 | | P. Ray | NRL | VT, NMT |
| Ionospheric Absorption Measurements using LWA1 as an Imaging Radiometer | 432 | 216 | L. Rickard | UNM | JPL, NRL |
| Single Dispersed Pulses | 320 | | J. Simonetti | VT | UMd, CWRU, CNJ |
| Observing the Transient Universe with the First LWA Station | | Cont. | G. Taylor | UNM | VT, NRL, JPL, LANL |
| Solar Radio Bursts at High Temporal and Spectral Resolution | 320 | 160 | S. White | AFRL | UNM, NRL, GMU, UMd, UTas |
| LEDA | 300 | | L. Greenhill | CfA | |
| Observing Cosmic Dawn with LWA1 | 520 | | J. Bowman | ASU | UNM |

Notes: These projects have already been allocated observing time in 2011/2012.

accepted that pulsars are rotating neutron stars, the pulsar emission mechanism and the geometry of the emitting region are still poorly understood (Eilek *et al.*, 2005). LWA1 will be an excellent telescope for the study of pulsars including single pulse studies and studies of the interstellar medium (ISM). In fact it is in LWA1 frequency band range where strong evolution in pulsar radio emission can be observed, e.g, a turn over in the flux density spectrum, significant pulse broadening, and complex changes in the pulse profile morphologies (Malofeev *et al.*, 1994). And, although pulsars were discovered at low frequency (B1919+21 at 81 MHz; Hewish *et al.*, 1968), there is a remarkable lack of observational data in the LWA1 frequency range. Figure 8 shows an LWA1 observation of B1919 + 21; and the LWA1 will detect dozens more (see Jacoby *et al.*, 2007) in less than 1000 s.

LWA1 is able to perform spectral studies of pulsars over a wide frequency range and with high

spectral resolution. This will allow investigators to look for drifting subpulses. Strong notches have been seen to appear in the profiles of pulsars at low frequencies (Hankins, 1973), but little progress has been made in understanding their origin. Some pulsars may reach 100% linear polarization at low frequencies (B1929 + 10; Manchester *et al.*, 1973). In addition to being intrinsically of interest (providing clues about the pulsar magnetospheric structure), such strongly polarized beacons can assist in probing coronal mass ejections and determining the orientation of their magnetic fields. That orientation can strongly influence their effects if they impact the Earth (Kassim *et al.*, 2010).

LWA1's large collecting area will be particularly useful for "single pulse" science, including studies of Crab giant pulses (CGPs; Bhat *et al.*, 2007) and anomalously intense pulses (AIPs; Stappers *et al.*, 2011). The Crab Pulsar intermittently produces single pulses having intensity greater than those

of the normal periodic emission by orders of magnitude. Despite extensive observations and study, the mechanism behind CGPs remains mysterious. Observations of the Crab pulsar across the electromagnetic spectrum can distinguish between various models for GP emission such as enhanced pair cascades, radio coherence, and changes in beaming direction. To date the study of the CGP emission at low radio frequencies is only very sparsely explored. Reported modern observations of CGPs in this frequency regime are limited to just a few in recent years including UTR-2 at 23 MHz (Popov *et al.*, 2006), MWA at 200 MHz (Bhat *et al.*, 2007), and LOFAR LBA (Stappers *et al.*, 2011). LWA1 will be able to provide hundreds of hours per year of sensitive observations of CGPs which could significantly increase our knowledge of the time- and frequency-domain characteristics of these enigmatic events.

We should be able to measure scattering for practically every good CGP detection (S/N \sim 20 or better), and it is known that both the dispersion and scattering of the Crab emission can vary dramatically on short or long time scales. By observing over an extremely broad bandwidth, we may be able to better quantify the scatter broadening and thereby assess the level and importance of anisotropy. Furthermore, the broad bandwidth of the observations will be helpful in shedding light on the issue of the frequency scaling of the scattering (believed to be \sim 3.6 compared to the canonical value of \sim 4.4 for the general ISM), which is thought to be related to the nature of turbulence in the nebula.

Anomalous high intensity single pulses from known pulsars have been reported previously using the UTR-2 (Ulyanov *et al.*, 2006) and LOFAR (Stappers *et al.*, 2011). These anomalously intense pulses (AIPs) have many features similar to the giant pulse phenomenon, including emission in a narrow longitude interval and power-law distribution of the pulse energy. One distinctive feature of these AIPs, however, is that they are generated by subpulses or some more short-lived structures within subpulses. The emission is seen to be quite narrow band, typically 1 MHz in bandwidth. The nature of such pulses is not yet understood. LWA1 with its excellent sensitivity and large available bandwidth provides an opportunity to study these pulses.

2.2. Hot jupiters

The magnetized planets in our solar system are well known to produce extremely bright coherent radio emission at low frequencies (e.g., Carr *et al.*, 1983). In the past decade, with the abundant detection of planets around other stellar systems, much theoretical work has been carried out on the detection of similar radio emission from extrasolar planets (e.g., Lazio *et al.*, 2009). Such a detection is the only currently viable method for measuring the magnetic fields and rotation rates of extrasolar planets, and it may provide information about the other properties, such as interior composition. For a terrestrial-mass planet, a magnetic field may be important for determining its habitability by protecting the planet from energetic particles. The brightest extrasolar planets are the Hot Jupiters (HJs), which we define as having semimajor axes less than 0.5 AU and masses above 0.5 Jovian masses.

Using LWA1, we will conduct a volume-limited search out to 50 pc for decametric emission from all known HJs in the northern hemisphere. The observational capabilities of LWA1 are uniquely suited to the properties of these sources:

- **Low-frequency coverage.** Decametric emission from a HJ will exhibit a sharp cutoff at the electron cyclotron frequency of the planet’s magnetic field, with typical cutoffs ranging from 1–100 MHz. The LWA1’s benign RFI environment allows observation down to 20 MHz routinely, and down to 10 MHz during favorable ionospheric conditions.
- **Sensitivity to polarized and “bursty” emission.** HJ emission is expected to be highly polarized and released in bursts with timescales of \sim 1 ms to \sim 10 s; LWA1 observations provide full Stokes parameters and better than 1 ms temporal resolution.
- **Extensive coverage of many targets.** The emission may be narrowly beamed, intersecting the Earth for a small fraction of the 10–100 hr rotational periods for some sources, while missing Earth entirely for others. The multiple independent beams of LWA1 allow us to dedicate approximately 300 beam-hours to begin this survey.
- **mJy sensitivity.** The large collecting area of LWA1 allows us to achieve a typical

(non-imaging) sensitivity of 10 mJy for each observation in our survey (of duration 14 hrs), lower than the ~ 100 mJy flux densities predicted for some HJs (Griessmeier *et al.*, 2007).

To date, searches below 70 MHz have had sensitivities of no better than 100 mJy (Zarka, 2007). After only six months of observation, we will either make a detection or be able to place tight constraints on models for HJ emission.

Additionally, LWA1 will be used to conduct *blind* searches for HJ emission. Based on stellar density estimates of the solar neighborhood (e.g., Howard *et al.*, 2010), we expect approximately 5,000 HJs within 100 pc. At a probable detection frequency of 20 MHz, an LWA1 beam is ~ 50 deg² at zenith (and larger still at lower altitudes), on average covering six nearby but unknown HJs. To detect these sources, we will add a search of bursty, highly polarized emission to our analysis of the beamformed data. Candidate detections will be followed up with dedicated observational programs to look for periodicity of such emissions, a sign that we have detected a HJ or similarly emitting brown dwarf.

2.3. Transients

Astrophysical transient sources of radio emission signal the explosive release of energy from compact sources (see Lazio *et al.*, 2010, Cordes & McLaughlin, 2003 for reviews). Known types of radio transients include cosmic ray airshowers, solar flares (Sec. 2.5), Jovian flares and flares from extrasolar Hot Jupiters (Sec. 2.2), giant flares from magnetars (Cameron *et al.*, 2005), rotating radio transients (McLaughlin *et al.*, 2006), giant pulses from the Crab pulsar (Sec. 2.1), and supernovae. The study of these sudden releases of energy allow us to recognize these rare objects, and yield insights to the nature of the sources including energetics, rotation rates, magnetic field strengths, and particle acceleration mechanisms. Furthermore, some radio transients remain unidentified such as the galactic center radio transient GCRT J1745-3009 (Hyman *et al.*, 2005), and require further study. A number of sources have been predicted to produce strong radio transients, but have not yet been observed, including prompt emission from gamma-ray bursts (GRBs; Benz & Paesold, 1998), neutron star mergers (Hansen & Lyutikov, 2001), expiration

of primordial black holes (Rees, 1977; Blandford, 1977), topological phase transitions in primordial black holes (Kavic *et al.*, 2008), and superconducting cosmic strings (Vachaspati, 2008).

A number of instruments have been built to study the meter-wavelength transient radio sky including the Cambridge Low Frequency Synthesis Telescope (Dessenne *et al.*, 1996), the Fallbrook Low-Frequency Immediate Response Telescope (FLIRT; Balsano, 1999), the Eight-meter Transient Array (ETA; Deshpande, 2009), and the Long Wavelength Demonstrator Array (LWDA; Lazio *et al.*, 2010). These surveys had limited collecting area, field-of-view, or availability. LWA1 will far surpass the limits set by these instruments, in sensitivity by two orders of magnitude, and with access to much of the sky all the time.

The Prototype All-Sky Monitor (PASI) is a software correlator and imager for LWA1 that analyzes the TBN data stream, which provides continuous samples from all dipoles with a 75 kHz passband placeable anywhere within 10–88 MHz (see Sec. 3). PASI images nearly the whole sky ($\approx 1.5\pi$ sr) every five seconds, continuously and in near realtime, with full Stokes parameters and typical sensitivities of ~ 5 Jy at frequencies above 40 MHz and ~ 20 Jy at 20 MHz. Candidate detections can be followed up within seconds by beamformed observations for improved sensitivity and localization. These capabilities provide an unprecedented opportunity to search the synoptic low-frequency sky. PASI saves visibility data for ~ 20 days, allowing it to “look back in time” in response to transient alerts. The images generated by PASI will be archived indefinitely.

LWA1 will also search for single dispersed pulses or cosmic “events” using beamforming mode. This mode trades all-sky capability for greater bandwidth and time resolution. Multiple beams will be used to mitigate against interference. In 50–70 MHz, any given coordinate will remain in the beam for about 14 min, which is sufficient to view the entire duration of pulses with DM up to ~ 1100 pc cm⁻³.

Ultimately, we plan for LWA1 to generate and accept alerts for multi-wavelength follow-up; its observations will be even more valuable in conjunction with the results of other facilities surveying large areas of the sky (e.g., Fermi, Pan-STARRS, LSST, LIGO). Furthermore, LWA1

is complementary to LOFAR in that the two instruments have little simultaneous overlap on the sky, but complimentary in that it has much better access to the Galactic center and inner plane where one might expect some transient populations to be concentrated (Kassim *et al.*, 2003).

2.4. Cosmic dawn and LEDA

Understanding the origin, formation, and evolution of the first galaxies is one of the major questions of astrophysics. Identified by the Astro2010 decadal review (New Worlds, New Horizons in Astronomy and Astrophysics) as an area ripe for exciting new discoveries, the period of “Cosmic Dawn” encompasses the formation of the first galaxies and black holes. These luminous sources produce UV and X-ray radiation that radically alters the properties of the diffuse neutral hydrogen gas that fills the majority of space at these times. It is crucial that we develop observational probes of this era since this would give valuable insights into the energetics of the early universe and the processes of initial

galaxy formation. One unique avenue for observationally constraining the radiative properties of the first luminous objects is via low frequency radio observations of the redshifted 21 cm line of neutral hydrogen (Madau *et al.*, 1997).

Coupling with the gas temperature results in the HI line being seen in absorption at high redshifts, when the gas is cooler than the CMB due to adiabatic expansion (during the so-called “Dark Ages”); it appears in emission at lower redshifts, after the gas becomes heated by X-rays from the first stars and black holes. According to theoretical models, the turnover between these regimes is around $z \sim 17$, at 80 MHz (Furlanetto *et al.*, 2006; Pritchard & Loeb, 2008), and the maximum absorption occurs between 50 and 100 MHz (Pritchard & Loeb, 2010). Figure 9 shows a theoretical model for the temperature history of the early universe, along with the predicted HI absorption signature.

Bowman and collaborators have proposed a novel approach to measuring the global 21 cm

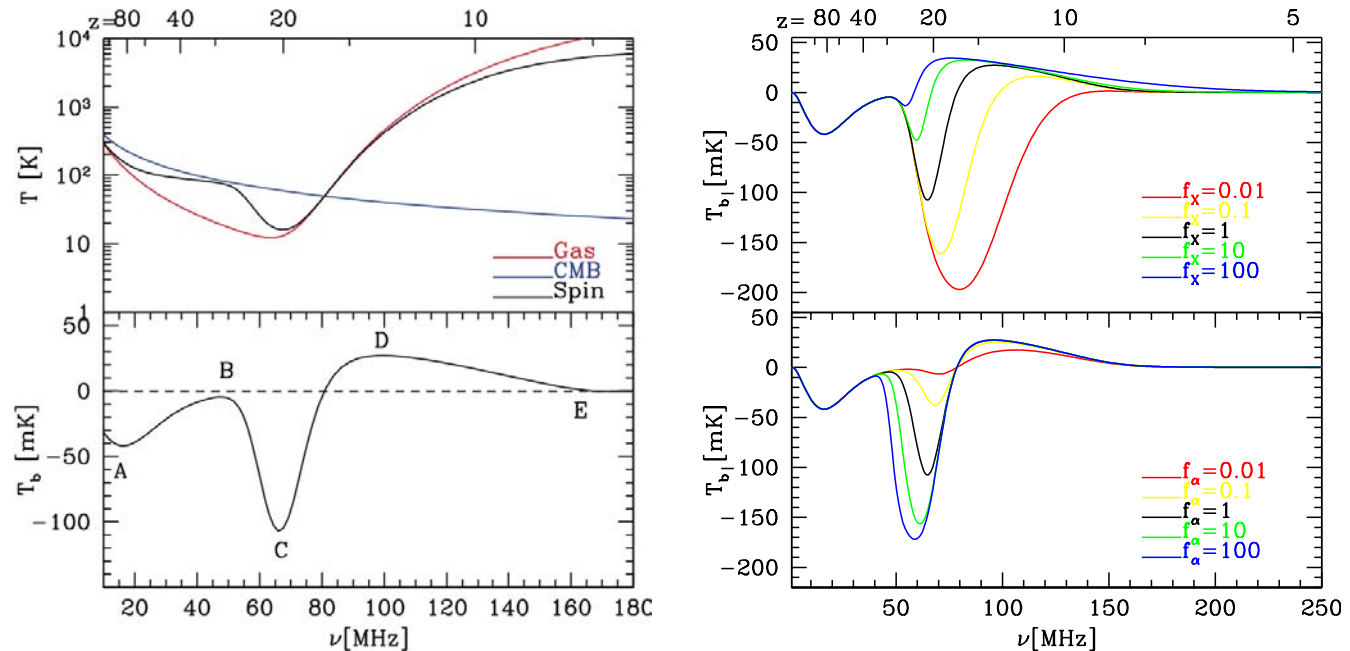


Fig. 9. (Color online) Evolution of temperature scales relevant for the 21 cm signal as a function of frequency. Top left panel: Evolution of the gas (red curve), CMB (blue curve), and spin (black curve) temperature for the fiducial history of Pritchard & Loeb (2010). Bottom left panel: Evolution of the 21 cm brightness temperature with inflection points (A,B,C,D,E) labeled. At (A) collisional coupling of the gas and spin temperature begins to become ineffective; at (B) Ly α photons begin to couple the gas and spin temperatures producing an absorption feature; at (C) X-rays from stars and/or galaxies heat the gas and eventually lead to an emission signature which peaks at (D); finally reionization removes all signal at (E). LWA1 will probe the regions from 20–84 MHz where the signal is in absorption. Right: Alternative scenarios for 21 cm heating from X-rays (top) and Ly α (bottom) which changes the strength of the absorption signal. Here f_x is the product of the X-ray emissivity and the star formation efficiency, and f_α is the product of the Ly α emissivity and the star formation efficiency.

signature using LWA1. They will detect or constrain the absorption peak that marks the end of the Dark Age using LWA1. LWA1 is well-matched to the expected frequency range of the absorption peak, and by simultaneously forming a science beam that targets a relatively cold region of sky and a strong source with a known spectrum, they will achieve a lower foreground and a better spectral calibration than single-antenna experiments allow. Furthermore, they will be able to repeat the experiment using different patches of sky, which further reduces the problem of foregrounds and allows for follow-ups of any marginal detections. This approach requires no additional hardware beyond what has already been developed for LWA1 and can be accomplished in ~ 500 beam hours.

Greenhill, Werthimer, Taylor, and Ellingson have proposed a more ambitious method to measure or constrain the HI signal from the transition between the Dark Ages and widespread reionization. The Large Aperture Experiment to Detect the Dark Ages (LEDA)^(b) comprises (i) a large-N correlator deployed to the LWA1 (512 inputs, 60 MHz), (ii) hardware to equip four outrigger dipoles for (redundant) calibrated total-power measurement, and (iii) a data calibration pipeline with which to reconstruct the full-Stokes sky brightness over a $\sim 140^\circ$ field of view, measure and correct for direction-dependent gains of individual stands, and measure and correct for refractive offsets created by the ionosphere (see Greenhill & Bernardi, 2012). In LEDA, the array will serve to enable calibrations that cannot be achieved with a single antenna; the outriggers will deliver the data streams from which the 21 cm science will be derived. The wide-band, wide-field sky model and antenna calibrations derived from array data will enable foreground subtraction (from the total power data). Use of multiple outriggers and a calibration array that can be subdivided to yield independent measurements will enable quantification of systematics. Cross-correlation for a large-N array scales as $O(N^2)$ and poses significant computing challenges. Hundreds of apertures and frequency channels, and tens of MHz bandwidth require 10^{13} to 10^{14} operations per second. The LEDA FX correlator will combine Field Programmable Gate Arrays (FPGAs) serving the $O(N)$ F stage and Graphics

Processing Units (GPUs) serving the $O(N^2)$ X stage (Clark, LaPlante, Greenhill, 2012). Application of GPUs, which may be coded in a C-like environment, reduced development time and cost while delivering nearly 80% utilization of the GPU floating point resources (single precision) and ready reconfigurability.

We note that detecting the 21 cm signal from the Dark Ages has many challenges to overcome including foreground subtraction, understanding sidelobe systematics, mitigating RFI and mutual coupling, and coping with ionospheric distortions. It could be that space-borne measurements are needed to bypass RFI and ionospheric effects. The Dark Ages Radio Explorer (DARE) mission (Burns *et al.*, 2012) has been proposed to deploy a radio telescope into an orbit around the moon to measure the Dark Ages signal.

2.5. Solar bursts

LWA1 will use single-beam measurements of the Sun, taking advantage of the sensitivity and temporal and spectral resolution available with LWA1, to look specifically at the fine structure in Type II and Type III bursts, and possibly to track moving Type IV bursts. The combination of sensitivity and time resolution will permit us to use the wave field statistics to test proposed models for the emission process. An example of this is shown in Fig. 10 taken during the solar event on 2011 Feb 14 using the TBN mode with 10 dipoles and the prototype LWA1 digital processor.

Type III bursts are generated by beams of nonthermal keV-energy electrons propagating out from the Sun on open field lines, producing radio emission at the local plasma frequency by plasma emission, i.e., conversion of electrostatic Langmuir waves into electromagnetic waves. Since the electrons are traveling rapidly outward into a plasma of decreasing density, the corresponding radio bursts drift rapidly downwards in frequency and appear as nearly vertical features in frequency-versus-time plots (“dynamic spectra”). The currently favored “stochastic growth” theory for plasma emission predicts a log-normal distribution for wave-field strengths in these bursts (e.g., Cairns & Robinson, 1999) that can be tested with LWA1 data. By contrast, Type II bursts are associated with shocks propagating through the solar corona. They are usually associated with coronal mass ejections,

^b<http://www.cfa.harvard.edu/LEDA/>

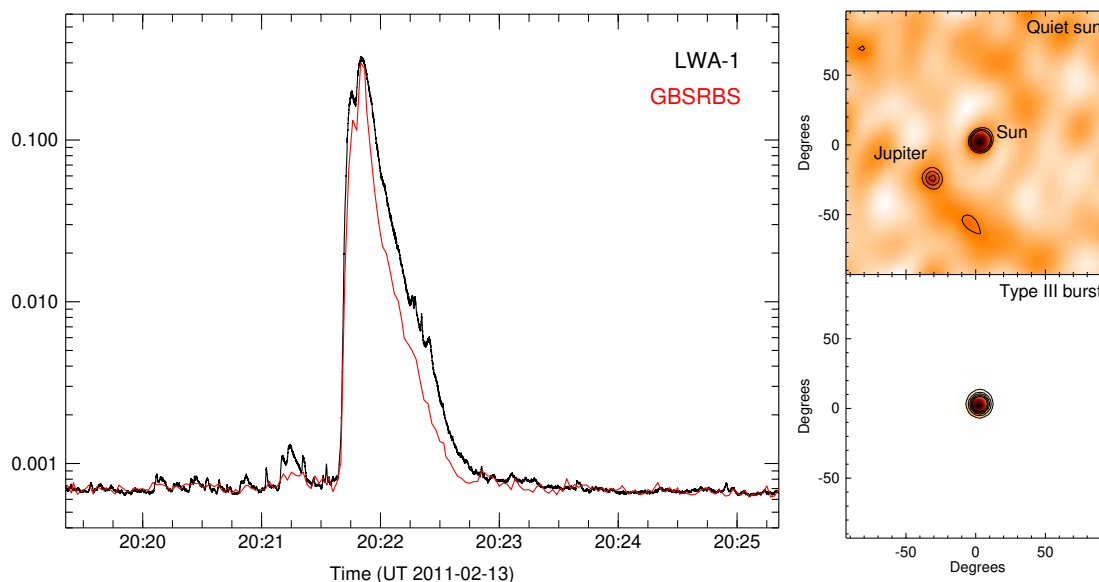


Fig. 10. (Color online) (Left) The 30 MHz light curve of a solar Type III burst at 0.04 s time resolution (bandwidth 50 kHz) from LWA1 (black line), compared with (red line) the 2 s time resolution, 2 MHz bandwidth light curve from the Green Bank Solar Radio Burst Spectrometer (GBSRBS; White *et al.*, 2005). The noise level in LWA1 data is much lower than in the GBSRBS data (from a single dipole antenna), and the low-level LWA1 variability is real. (right) Comparison of LWA1 maps of the sky centered on the Sun before the burst (upper, 2011 Feb 13 at 20:19:20 UT) and near the peak of the burst (lower, 20:21:50 UT). Both maps contain a few seconds of data and use 4 kHz of bandwidth. The maps were made using data from just 8 dipoles relatively close to each other in LWA1. The resolution is 10 degrees. The peak in the burst map is about 5000 times brighter than the peak in the pre-burst map.

which can generate shocks as they move through the solar atmosphere at high speed. However, there are aspects of Type II bursts that appear to be correlated with the structure of the flaring region itself. Type II bursts show much substructure in frequency-time plots that may be associated with inhomogeneity in the shock, and with the mechanism for generation of Langmuir waves. The exact nature of the source of plasma emission in Type II bursts is still not entirely understood: it could be due to widespread electron beams, as in Type III bursts, but this is more likely to be true of the structures known as “herringbone”, short-lived fast-drift structures seen to emerge from the backbone of Type II emission. LWA1 data sampled at high temporal and spectral resolution may give clues to acceleration processes in the shock creating the burst. Moving Type IV bursts are associated with large solar eruptions and can move several degrees at thousands of km/s: in extreme cases LWA1’s high signal-to-noise should permit it to measure such motions even with the large beam and reinvigorate a field of study that has been largely dormant for 20 years due to the lack of imaging at LWA1’s

frequencies where these intriguing (and potentially space-weather relevant) phenomena occur.

2.6. Radio recombination lines

Radio recombination lines (RRLs) arise in ionized and partially ionized gas, and therefore offer valuable probes of the physical condition of the diffuse ionized interstellar medium. In particular, the size of the electron orbit increases for high quantum numbers, making the particles extremely sensitive to temperature and density of the medium. At LWA1 frequencies the excitation temperature approaches the kinetic temperature and RRLs are expected to be seen in absorption, confirmed by carbon RRL detections (Fig. 11; Stepkin *et al.*, 2007; Kantharia & Anantharamaiah, 2001; Erickson *et al.*, 1995). Hydrogen RRLs at these frequencies are as yet undetected, perhaps due to a dielectronic electron capture mechanism increasing the chance of absorption in atoms with multiple electrons such as carbon (Walmsley & Watson, 1982).

Our knowledge of carbon (and other species) RRLs is currently relatively limited, and LWA1

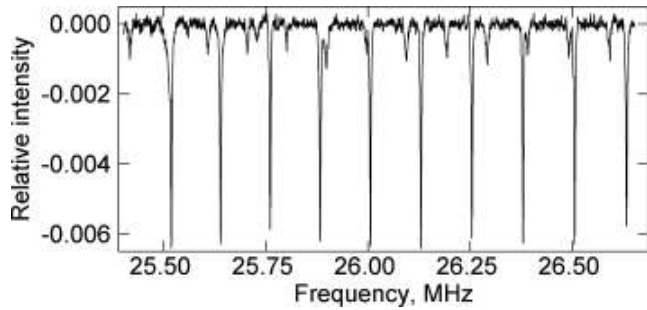


Fig. 11. The spectrum of carbon at 26 MHz taken in the direction of Cas A (Stepkin *et al.*, 2007).

opens up a new venue for observations of these lines. In particular, the versatile bandwidth and spectral resolution will be essential for successful observations of RRLs (Peters *et al.*, 2011). For example, at frequencies ~ 26 MHz the spectral resolution required to separate between the carbon RRLs is ~ 125 kHz (see Fig. 11). At the same time, a large bandwidth is desired since then many lines can be observed at the same time, and the resulting spectra can be folded to search for a possible detection. Using three beams at LWA1 we can simultaneously cover about 85 carbon transitions with a 0.5 kHz spectral resolution (6 km/s). This is straightforward for LWA1 because the native format for data recording is voltage samples, as opposed

to spectrometer output; channelization can be performed in software at any desired frequency resolution. The 100-m aperture size of LWA1 also offers improved angular resolution over single-dish studies (Erickson *et al.*, 1995).

The first approved RRL observing project (see Table 3) includes proof-of-concept observations of the known lines in Cas A to work out any necessary calibration and reduction procedures. Once these are established, three targets in the Cygnus Arm have been selected as suitable places for an initial RRL search. The three targets are DR21 (HII region), HB21 (supernova remnant) and DR4 (supernova remnant), all of which are bright at low radio frequencies and are likely to contain large amounts of ionized or partly ionized gas. Future possible and obvious RRL studies with LWA1 include surveys of large regions to map the conditions of the diffuse ISM, and searches for other RRL species.

3. Observatory Description

LWA1 lies on NRAO property, just a few hundred meters southwest of the center of the VLA (see Fig. 1). The LWA1 system architecture is shown in Fig. 12. The array consists of 258 active antenna stands. All but two of the antennas are located within an ellipse of 100 m (East–West) \times 110 m

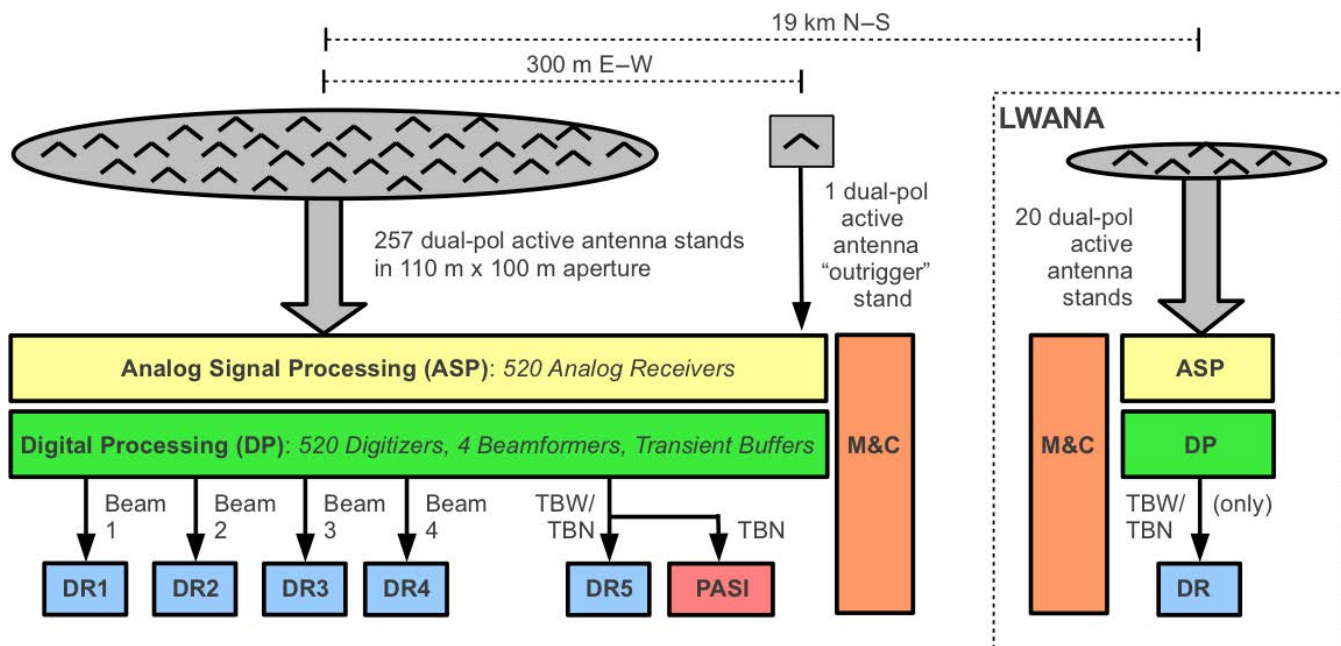


Fig. 12. LWA1 system architecture, simplified for clarity; details available in Craig (2009).

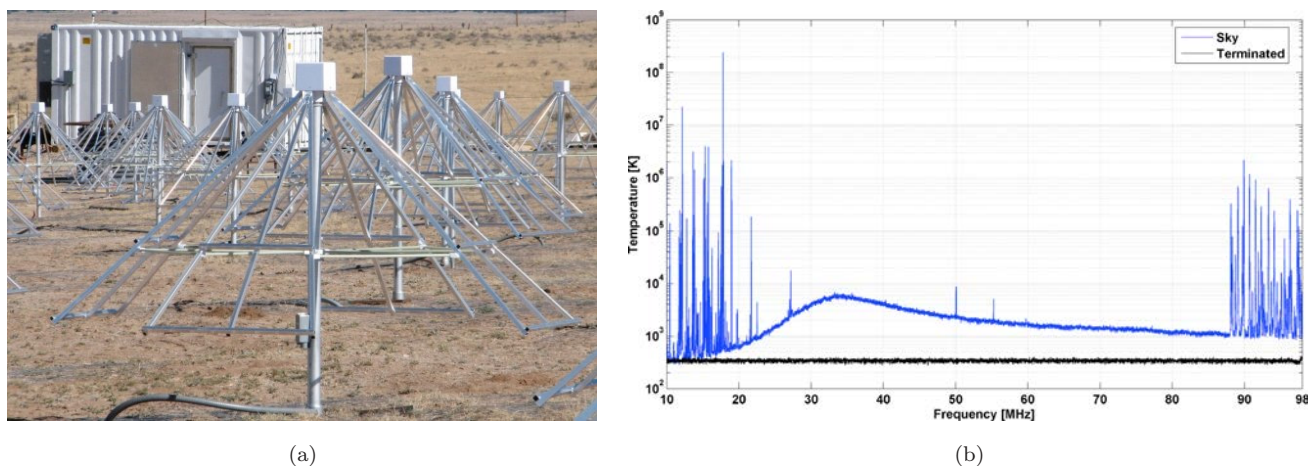


Fig. 13. LWA1 active antenna. (a) An active antenna “stand”, consisting of two orthogonally-aligned bowtie-type dipoles on a mast, over a $3\text{ m} \times 3\text{ m}$ ground screen. (b) Output spectrum of one polarization of the active antenna and output with antenna terminals shorted, confirming that the output is sky noise-dominated over most of the 10–88 MHz tuning range.

(North–South), with the axial ratio intended to improve beam shape for pointings toward the Galactic Center, which transits at $Z \approx 63^\circ$ as seen from the site. The other two stands are outliers (one 77 m SW of center, and one 300 m E of center) used primarily for calibration and diagnostic purposes. Additional outliers are planned as part of the LEDA project.

An LWA1 antenna stand is shown in Fig. 13(a). Integral to the stand is an “active balun” that provides about 35 dB of gain to overcome subsequent losses, ensuring that the system temperature is dominated by Galactic (*not* internal) noise, as demonstrated in Fig. 13(b). Upon arrival in the shelter, the signal from every antenna is processed by a direct-sampling receiver consisting of an analog receiver, a 12-bit analog-to-digital converter (A/D) which samples 196 million samples per second (MSPS), and subsequent digital processing (“DP”) (see Fig. 14(b)). This choice of sample rate ensures that strong RFI from the 88–108 MHz FM broadcast band aliases onto itself, with no possibility of obscuring spectrum in the 10–88 MHz tuning range. Beams are formed using a fully-digital time-domain delay-and-sum architecture, which allows the entire 78 MHz passband associated with each antenna to be processed as a single data stream (Soriano *et al.*, 2011). Delays are implemented in two stages: An integer-sample “coarse” delay is applied using a first-in first-out (FIFO) buffer operating on the A/D output samples, followed by a 28-tap finite impulse

response (FIR) filter that implements an all-pass “subsample” delay. The filter coefficients can be also specified by the user, allowing the implementation of beams with custom shapes and nulls. The delayed signals are added to the signals from other antennas processed similarly to obtain beams. Four dual-polarization beams are constructed in this fashion, each fully-independent and capable of pointing anywhere in the visible sky. Each beam is subsequently converted to two independent “tunings” of up to ≈ 16 MHz bandwidth each, with each tuning having a center frequency independently-selectable from the range 10–88 MHz. Both tunings of the beam emerge from DP as a single stream of UDP packets on 10 Gb/s ethernet. Thus there is one 10 Gb/s ethernet output cable per beam (or “pointing”).

Each beam output is connected to a data recorder, a PC that records the UDP packets to a “data recorder storage unit” (DRSU). A DRSU is five 2 TB drives (10 TB total) in a 1U rack-mountable chassis, configured as an eSATA drive array. Each data recorder can host up to two DRSUs. At the maximum beam bandwidth, each data recorder has a capacity of ≈ 72 hrs of observation which is continuous except for one gap of approximately 5 min, needed for the switchover between DRSUs. DRSUs may be either taken from the shelter for analysis, or they may be offloaded onto other DRSUs or commercially-available external USB hard drives. It is also possible to transfer data from data recorders directly off-site using the internet; however the limited data

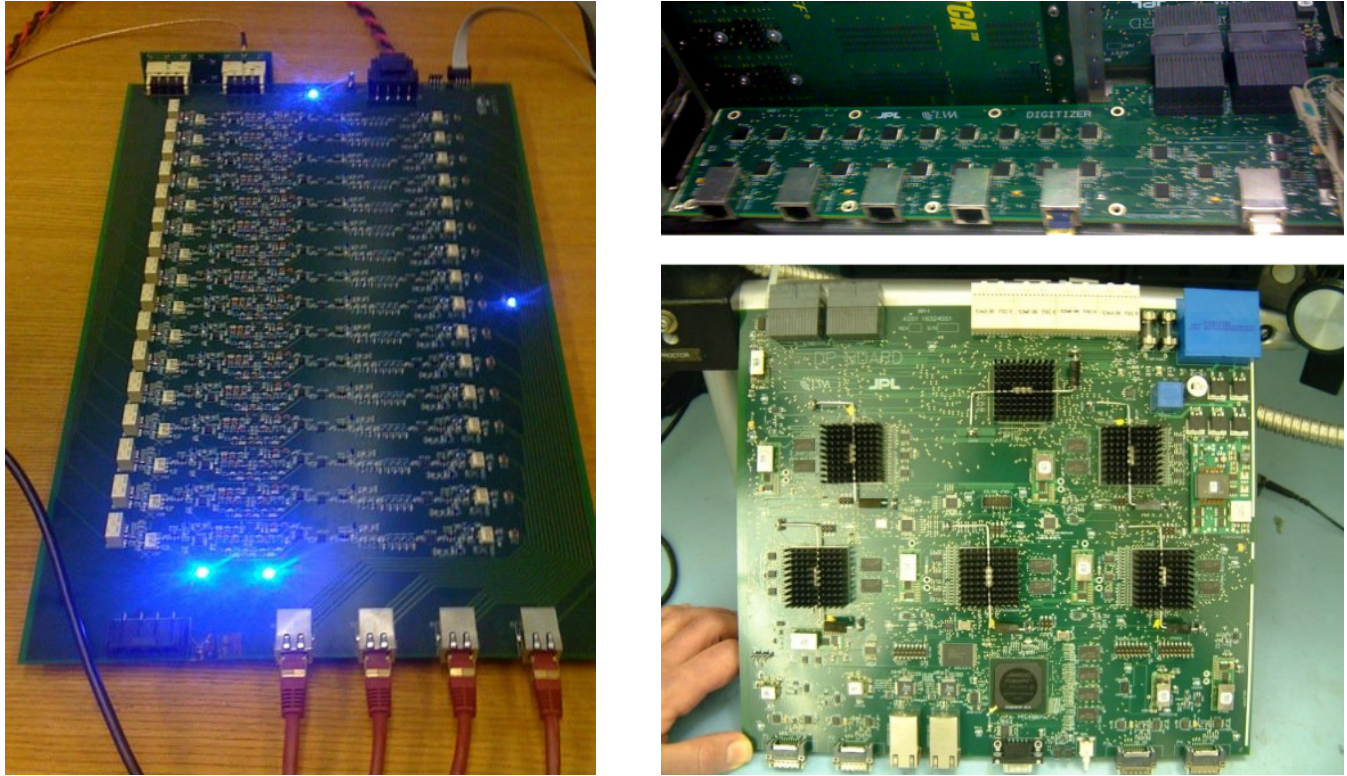


Fig. 14. Left: One of LWA1’s 33 16-channel analog receiver boards. Top Right: One of the digitizer boards; Bottom Right: One of LWA1’s 26 20-channel “DP1” digital processing boards. Note the 5 FPGAs on the DP1 boards which are Xilinx Vertex V series.

rate of the internet connection to the LWA1 site makes this impractical for observations longer than a few minutes.

Independently of beamforming, and as demonstrated in Figs. 2–4, LWA1 is able to coherently capture and record the output of all its A/Ds, where each A/D corresponds to one antenna. This can be done in two distinct modes. The “transient buffer — wideband” (TBW) mode allows the raw 12-bit output of the A/Ds to be collected continuously, but only for 61 ms at a time, and another 5 min is required to write out the captured samples. The “transient buffer — narrowband” (TBN) mode, in contrast, allows a single tuning of 75 kHz bandwidth to be recorded continuously and indefinitely, resulting in an output data rate of ~ 112 MB/s for the array. These two modes share the same 10 Gb/s ethernet output from DP, and thus are mutually exclusive. However, the TBW/TBN output is distinct from the four beam outputs and runs simultaneously with all four beams using a dedicated (fifth) data recorder and DRSUs. Although intended originally to support commissioning and diagnostic

functions, the TBW and TBN modes have emerged as popular modes for science observations, as indicated in Sec. 2.

LWA1 includes a dedicated backend known as the Prototype All-Sky Imager (PASI). PASI shares the TBN/TBW output and operates $\sim 80\%$ of the observatory uptime. PASI is a cluster of 4 rack mounted servers with Nahalem multicore processors interconnected by an Infiniband switch.

Separate from LWA1, we have built the LWA North Arm stub station (LWANA), a separate station located at the end of the VLA’s North Arm (approximately 19 km North of LWA1) primarily using spares left over from the original procurements of components for LWA1. LWANA consists of 20 stands (thus, $\sim 8\%$ of the collecting area of LWA1) and is capable of TBW and TBN only (not beamforming). However, it is identical to LWA1 in all other respects, including data recording.

Radio frequency interference (RFI) environment: As demonstrated in Figs. 3, 5, 7, and 13(b), the RFI environment at LWA1 is

surprisingly benign. The observatory management team has had extensive experience — and consistent success — observing at these frequencies at this site using LWA1, a precursor system (LWDA; Lazio *et al.*, 2010), and the VLA 4-m system (Kassim *et al.*, 2007a). This is not to say that observing in 10–88 MHz is without challenges. RFI impacts LWA1 on two levels: First, by creating a potential threat to the linearity of the active antennas and analog receivers; and second, by obstructing the spectrum/spectra of interest. We consider the linearity issue first. At LWA1, the most troublesome interference is due to distant transmitters at frequencies below about 30 MHz, whose signals arrive at the station by refraction from the ionosphere, followed closely by FM broadcast signals in the 88–108 MHz range. These linearity challenges are met using high-intercept point active front end electronics in which we have great confidence (the same design with only minor modifications has been in nearly continuous use at the site since 2006). Also the LWA1 analog receivers (Fig. 14(a)) can be electronically reconfigured between three modes: A full-bandwidth (10–88 MHz) uniform gain mode, a full-bandwidth dual-gain mode in which frequencies below about 40 MHz can be attenuated using a “shelf filter” (useful for observing above 40 MHz during that part of the day when long-range signals in the 10–30 MHz band are strongest); and a 28–54 MHz mode, which would serve as a last line of defense should we find in the future that RFI above and/or below this range becomes persistently linearity-limiting. In addition, the total gain in each bandpass mode can be adjusted over a 60 dB range in 2 dB steps, allowing fine adjustments to optimize the sensitivity-linearity tradeoff.

Concerning the obscuration of science signals from in-band RFI: Our extensive experience in this frequency range (from the 74 MHz VLA system, from LWDA and ETA, and from LWA1 itself) has demonstrated that RFI from both external and internal sources will inevitably be present at all levels and throughout the spectrum. We occasionally encounter bouts of crippling interference, which we inevitably find to be internally generated, from local powerlines, or due to activity at the nearby VLA facilities. In each case we have (with the excellent cooperation from the VLA RFI management team) quickly identified and eliminated the source. For the remaining low-level RFI, we find

that the simple time & frequency editing techniques currently employed are effective in dealing with interference encountered most of the time. In fact, we typically find that the primary difficulty posed by RFI is not really that it prevents science, but rather that it increases the amount of manual effort required to reduce data, and decreases somewhat the amount of data that is ultimately useful.

We plan a continuing program of technical development aimed at characterizing, expanding and improving the capabilities of LWA1 and, in the process, training students in the art of instrument development and developing the engineering expertise needed to tackle the next generation of large meter-wavelength radio telescopes. The LWANA (see Sec. 3) is available as a testbed for technical development projects, so that work can proceed with less concern about inadvertently degrading LWA1 with unproven modifications, or limiting its availability to accommodate testing. Technical developments planned include: (1) On-the-fly data processing using the existing data recorders; (2) Flexible scheduling, triggering, and rescheduling of observations; (3) Enhanced and automated techniques for mitigation of RFI; (4) Beams with custom shapes and/or optimized sensitivity; and (5) Improved sidelobe and polarization characterization.

4. Observatory Operations

4.1. Allocation of observing time

LWA1 observing time is allocated in units of “beam-hours” and “TB-hours”. One beam-hour corresponds to the dedicated use of one of LWA1’s four independently-steerable beams for one hour. Similarly, one TB-hour corresponds to the dedicated use of LWA1’s TBW/TBN mode for one hour. Data will be shipped to users on hard drives, or made available online through the LWA Data Archive (LDA), a 24 TB online archive hosted at UNM’s Center for Advanced Research in Computing.

The first LWA1 CFP was conducted in October 2009, and resulted in the time allocations identified in Table 3. CFPs will be issued twice annually. LWA1 also supports “target of opportunity” observing. The Director (or in his absence, the Associate Director or Chief Scientist) is authorized to grant up to 16 beam-hours (sufficient to cover the full tuning range of LWA1 continuously for

one pointing, for 4 hrs) and 8 TB-hours in response to a well-justified email request from anyone.

Finally, it should be noted that the LDA will provide, in effect, a retroactive observing capability that we will also make available to the community.

4.2. The LWA software library

The LWA project has developed a suite of software tools for the scheduling and analysis of LWA data (the LWA Software Library — LSL, Dowell *et al.*, 2012; and see,^(c) but we do not have the resources to provide turn-key software solutions for all experiments that could be envisaged. We have established a clearinghouse for LWA Software and this will be available to all users. LSL initially benefited from a software repository developed by NRL for the LWDA, and software development at Virginia Tech. LSL runs under Linux and also on Intel Macs. Currently LSL includes readers for all LWA observing modes, correlators for the TBW and TBN dipole modes, and various scripts to generate plots of antenna locations, spectra, spectrograms, and more. LSL is publicly available from the LWA web pages.

5. Conclusions

LWA1 offers considerable sensitivity and sky coverage in the relatively unexplored frequency range 10–88 MHz. LWA1 is particularly interesting from an education perspective in that the TBN/TBW modes provide one of the first “Large-N” radio telescopes, challenging existing algorithms. Furthermore, there are a number of other low frequency instruments under commissioning and development (LOFAR, MWA, PAPER) which face similar challenges in RFI mitigation, calibration, and wide-field imaging.

The astronomical community is invited to apply for time on this new facility at one of the upcoming proposal deadlines.

Acknowledgments

We acknowledge the efforts of the following students and postdocs who helped to design or build LWA1: Sunil Danthuluri, Albino Gallardo, Sudipta Ghorai, Aaron Gibson, Eduard Gonzalez, Mahmud Haun, Aaron Kerkhoff, Ted Jaeger, Kyehun Lee, Justin

Linford, Qian Liu, Adam Martinez, Frank Schinzel, Abirami Srinivasan, D. W. Taylor III, Chenoa Tremblay, Steve Tremblay, Sushrutha Vignanam, Chris Wolfe, Jayce Dowell, Jake Hartman, Bryan Jacoby, Ted Jaeger, and Nagini Paravastu. Basic research in radio astronomy at the Naval Research Laboratory is supported by 6.1 base funding. GBT acknowledges support from the Lunar University Network for Astrophysics Research (LUNAR) (<http://lunar.colorado.edu>), headquartered at the University of Colorado Boulder, funded by the NLSI via Cooperative Agreement NNA09DB30A. Part of this research was carried out at the Jet Propulsion Laboratory, California Institute of Technology, under a contract with the National Aeronautics and Space Administration. The Centre for All-sky Astrophysics is an Australian Research Council Centre of Excellence, funded by grant CE11E0090. Construction of the LWA has been supported by the Office of Naval Research under Contract N00014-07-C-0147. Support for operations and continuing development of the LWA1 is provided by the National Science Foundation under grant AST-1139974 of the University Radio Observatory program.

References

- Balsano, R. J., 1999, PhD thesis, Princeton Univ.
- Benz, A. O. & Paesold, G., 1998, *A&A*, **329**, 61.
- Bhat, N. D. R. *et al.*, 2007, *ApJ*, **665**, 618.
- Blandford, R. D., 1977, *MNRAS*, **181**, 489.
- Burns, J. O., Lazio, J., Bale, S. *et al.*, 2012, *Advances in Space Research*, **49**, 433.
- Cairns, I. H. & Robinson, P. A., 1999, *PRL* **82**, 3066.
- Cameron, P. B. *et al.*, 2005, *Nature*, **434**, 1112.
- Carr, T. D., Desch, M. D. & Alexander, J. K., 1983, in *Physics of the Jovian magnetosphere*, eds. Dessler, A. J., New York: Cambridge University Press, 226–284.
- Clark, M. A., LaPlante, P. C. & Greenhill, L. J., 2012, *Intl. J. High Perf. Computing*, in press.
- Clarke, T., 2009, Scientific requirements for the long wavelength array, Memo 159, LWA Memo Series <http://www.ece.vt.edu/swe/lwa/>.
- Cordes, J. M. & McLaughlin, M. A., 2003, *ApJ*, **596**, 1142.
- Craig, J., 2009, Long wavelength array station architecture, Ver. 2.0, Memo 161, LWA Memo Series <http://www.ece.vt.edu/swe/lwa/>.
- Deshpande, K. B., 2009, *A Dedicated Search for Low Frequency Radio Transient Astrophysical Events using ETA*, M.S. Thesis, Virginia Polytechnic Institute and State University.
- Dessenne, C. A.-C. *et al.*, 1996, *MNRAS*, **281**, 977.
- de Oliveira-Costa, A., Tegmark, M., Gaensler, B. M., Jonas, J., Landecker, T. L. & Reich, P., 2008, *MNRAS*, **388**, 247.

^c<http://fornax.phys.unm.edu/lwa/trac/wiki>.

- de Vos, M., Gunst, A. W. & Nijboer, R., 2009, The LOFAR telescope: System architecture and signal processing, *Proc. IEEE*, **97**, 1431.
- Dowell, J., Wood, D., Stovall, K., Ray, P. S., Clarke, T. & Taylor, G. B., 2012, *JAI*, submitted.
- Eilek, J., Hankins, T. & Jessner, 2005, *ASP Conf. Ser.* **345**, 499.
- Ellingson, S. W., Clarke, T. E., Cohen, A., Craig, J., Kassim, N. E., Pihlstrom, Y., Rickard, L. J. & Taylor, G. B., 2009, The long wavelength array, *Proc. IEEE*, **97**(8), 1421–1430.
- Ellingson, S. W., 2011, Sensitivity of antenna arrays for long-wavelength radio astronomy, *IEEE Trans. Ant. & Prop.* **59**, 1855, astro-ph/1005.4232.
- Erickson, W. C., McConnell, D. & Anantharamaiah, K. R., 1995, *ApJ* **454**, 125.
- Furlanetto, S. R., Oh, S. P. & Briggs, F. H., 2006, *PhR*, **433**, 181.
- Griessmeier, J., Zarka, P. & Spreuw, H., 2007, *A&A*, **475**, 359.
- Hankins, T., 1973, *ApJ*, **181**, L49.
- Hansen, B. M. S. & Lyutikov, M., 2001, *MNRAS*, **322**, 695.
- Helmholtz, J. F. & Kassim, N. E., 2009, *AJ*, **138**, 838.
- Hewish, A., Bell-Burnell, J., Pilkington, J. D. H., Scott, P. F. & Collins, R. A., 1968, *Nature*, **217**, 709.
- Howard, A. W., Marcy, G. W., Johnson, J. A., Fischer, D. A., Wright, J. T., Isaacson, H., Valenti, J. A., Anderson, J., Lin, D. N. C. & Ida, S., 2010, *Science*, **330**, 653.
- Hyman, S. D., Lazio, T. J. W., Kassim, N. E., Ray, P. S., Markwardt, C. B. & Yusef-Zadeh, F., 2005, *Nature*, **434**, 50.
- Jacoby, B. A., Lane, W. M. & Lazio, T. J. W., 2007, Simulated LWA-1 pulsar observations Memo 104, LWA Memo Series <http://www.ece.vt.edu/swe/lwa/>.
- Kantharia, N. G. & Anantharamaiah, K. R., 2001, *JApA*, **22**, 51.
- Kassim, N. E., Perley, R. A., Erickson, W. C. & Dwarakanath, K. S., 1993, *AJ* **106**, 2218.
- Kassim, N. E. & Erickson, W. C., 1998, *SPIE*, **357**, 740.
- Kassim, N. E., Lazio, T. J. W., Nord, M., Hyman, S. D., Brogan, C. L., LaRosa, T. N. & Duric, N., 2003, in *Proceedings of the Galactic Center Workshop 2002 — The central 300 parsecs of the Milky Way*, *Astronomische Nachrichten*, **324**(S1), 73–78.
- Kassim, N., Perez, M., Junor, W. & Henning, P., eds., From clark lake to the long wavelength array: Bill Erickson's radio science, *ASP Conference Series*, **345**, 2005 Astronomical Society of the Pacific, San Francisco.
- Kassim et al., 2006, LWA1+ Scientific requirements Memo 70, LWA Memo Series <http://www.ece.vt.edu/swe/lwa/>.
- Kassim, N. E. et al., 2007a, The 74 MHz System on the Very Large Array, *Astrophys. J. Supp. Ser.* **172**, 686–719.
- Kassim, N. E. et al., 2010, The long wavelength array (LWA): A large HF/VHF array for solar physics, ionospheric science, and solar radar, *Proc. Advanced Maui Optical and Space Surveillance Technologies Conf.*, Sept 14–17, 2010, Maui, Hawaii. Also available as LWA Memo 172.
- Kavic, M., Simonetti, J. H., Cutchin, S. E., Ellingson, S. W. & Patterson, C. D., 2008, Transient pulses from exploding primordial black holes as a signature of an extra dimension, *J. Cosmology & Astroparticle Physics*, **11**, 017 <http://stacks.iop.org/1475-7516/2008/i=11/a=017>.
- Lazio, J., Bastian, T., Bryden, G., Farrell, W. M., Griessmeier, J., Hallinan, G., Kasper, J., Kuiper, T., Lecacheux, A., Majid, W., Osten, R., Shklorik, E., Stevens, I., Winterhalter, D. & Zarka, P., 2009, *Astro2010 whitepaper* arXiv:0903.0873.
- Lazio, T. J. W. et al., 2010, Surveying the dynamic radio sky with the long wavelength demonstrator array, *AJ*, **140**, 1995.
- Madau, P., Meiksin, A. & Rees, M. J., 1997, *ApJ*, **475**, 429.
- Malofeev, V. M., Gil, J. A., Jessner, A. et al., 1994, *A&A*, **285**, 201.
- Manchester, R. N., Taylor, J. H. & Huguenin, G. R., 1973, *ApJL*, **179**, L7.
- McLaughlin, M. A. et al., 2006, *Nature*, **439**, 817.
- Obenberger, K. & Dowell, J., 2011 LWA1 RFI survey Memo 183, LWA Memo Series <http://www.ece.vt.edu/swe/lwa/>.
- Perley, R. A. & Erickson, W. C., 1984, A proposal for a large, low frequency array located at the VLA site, Memo 1, LWA Memo Series <http://www.ece.vt.edu/swe/lwa/>.
- Peters, W. M., Lazio, T. J. W., Clarke, T. E., Erickson, W. C. & Kassim, N. E., 2011, *A&A*, **525**, 128.
- Popov, M. V. et al., 2006, *Astron. Rep.*, **50**, 562.
- Pritchard, J. R. & Loeb, A., 2008, *Phys. Rev. D*, **78**, 103511.
- Pritchard, J. R. & Loeb, A., 2010, *Phys. Rev. D*, **82**, 023006.
- Ransom, S. M., 2001, Ph.D. Thesis.
- Rees, M. J., 1977, *Nature*, **266**, 333.
- Rickard L. J. et al., 2010, The long wavelength array (LWA): A large HF/VHF array for solar physics, ionospheric science, and solar radar, Ground-based instrument paper for the 2010 NRC decadal survey of solar and space physics, Memo 173, LWA Memo Series <http://www.ece.vt.edu/swe/lwa/>.
- Soriano, M., Navarro, R., D'Addario, L., Sigman, E. & Wang, D., 2011, Implementation of a digital signal processing subsystem for a long wavelength array station, *Proc. 2011 IEEE Aerospace Conf, Big Sky, MT*. Also available as LWA Memo 179.
- Stepkin, S. V. et al., 2007, *MNRAS*, **374**, 852.
- Stappers, B. W. et al., 2011, *A&A*, **530**, A80.
- Ulyanov, O. M., Zakharenko, V. V., Konovalenko, A. A., Lecacheux, A., Rosolen, C. & Rucker, H. O., 2006, *IAU Joint Discussion*, **2**.
- Vachaspati, T., 2008, *Physical Review Letters*, **101**, 141301.
- Walmsley, M. & Watson, W. D., 1982, *ApJ*, **260**, 317.
- White, S., 2005, in From clark lake to the long wavelength array: Bill Erickson's radio science, Kassim, N., Perez, M., Junor, W. & Henning, P., eds., *ASP Conference Series*, **176**, 345 Astronomical Society of the Pacific, San Francisco.
- Wijnholds, S. J. & van Cappellen, W. A., 2011, *IEEE Trans. Ant. & Prop.*, **59**, 1981.
- York, J. et al., 2007 The LWDA array: An overview of the design, layout and initial results Memo 93, LWA Memo Series <http://www.ece.vt.edu/swe/lwa/>.
- Zarka, P., 2007, *Planet. Space Sci.*, **55**, 598.